Applied Mathematical Modelling 113 (2023) 309–332

Contents lists available at ScienceDirect

Applied Mathematical Modelling

journal homepage: www.elsevier.com/locate/apm

Modal sensitivity of three-dimensional planetary geared rotor systems to planet gear parameters

Ali Tatar[a,*], Christoph W. Schwingshackl[b], Michael I. Friswell[c]

[a] University of Bristol, Department of Aerospace Engineering, Bristol, BS8 1TR, UK
[b] Imperial College London, Department of Mechanical Engineering, London, SW7 2AZ, UK
[c] Swansea University, Faculty of Science and Engineering, Swansea, SA1 8EN, UK

ARTICLE INFO

Article history:
Received 8 February 2022
Revised 13 September 2022
Accepted 15 September 2022
Available online 18 September 2022

Keywords:
Geared rotors
Planetary gearbox
Modal analysis
Parameter effects
Vibration sensitivity

ABSTRACT

A parameter study is presented to determine effects of planet gear design parameters on the global modal behaviour of planetary geared rotor systems. The modal sensitivity analysis is conducted using a three-dimensional dynamic model of a planetary geared rotor system for the number of planet gears, planet mistuning, mass of planet gears, gear mesh stiffness and planet gear speed. These parameters have varying impacts on both natural frequencies and mode shapes, therefore the sensitivity of the planetary geared rotor vibration modes to the planet gear parameters is determined by computing the frequency shifts and comparing the mode shapes. The results show that the mass and mesh stiffness of planet gears have a larger influence on the global dynamic response. Torsional modes and coupled torsional-axial modes are more sensitive to gear mesh stiffness whereas lateral vibration modes are more sensitive to gearbox mass. Planet mistuning results in coupling between lateral and torsional vibrations. The planetary gearbox becomes more rigid in the torsional-axial modes and more flexible in the lateral modes with an increase in the number of planet gears. Planet gears are also found to be having significant gyroscopic effects inside the planetary gearbox. The main original findings in this study can be directly used as initial guidelines for planetary geared rotor design.

1. Introduction

Planetary gearboxes are used extensively in many industries such as aerospace [1,2], automotive [3] and marine [4] because of their higher power transmission capacity. The installation of a planetary gearbox into a rotating system introduces coupled dynamic problems which includes the dynamics of the gearbox and the whole rotor system, making the prediction of the dynamic, vibration and acoustic response of a geared rotor system somewhat challenging. Basically, a planetary gearbox can affect the vibrational behaviour of the rotor system with its mass and inertia, stiffness and damping, and gyroscopic moments.

Early papers on planetary gearbox dynamics research mostly focused on dynamic loads, stress and torsional vibrations in the 1970s and 1980s [5–12]. Purely torsional [13–16], torsional-transverse [17–20] and three-dimensional (including

* Corresponding author.
E-mail address: ali.tatar@bristol.ac.uk (A. Tatar).

https://doi.org/10.1016/j.apm.2022.09.021

Nomenclature

q	Generalized coordinates
ρ_p	Material density of planet gears
N	Number of planets
$\mathbf{\Omega}$	Rotating speed of elements
rpm	Revolution per minute
T	Kinetic energy
V	Potential energy
L	Total energy
ε	Modal energy ratio

Subscripts

$h = r, c, s$	Central member index
r	Ring gear
c	Carrier
s	Sun gear
p	Planet gear

torsional, transverse, tilting and axial motions) models [21–26] were then developed for the dynamic and modal analyses of planetary gearboxes. Recently, numerically identified modal behaviour of the planetary gearboxes have been validated with several experimental and operational modal analysis studies [20,27–30]. Furthermore, the planetary gearbox parameters such as load, mesh stiffness, bearing stiffness, mass and inertia, gear eccentricity and planet mistuning have been extensively analysed to investigate the parameter effects on the modal behaviour of planetary gearboxes themselves [31–40].

To understand the parameter effects on the dynamic and modal behaviour of geared rotor systems, researchers have mostly focused on stiffness and gyroscopic parameters in the literature [41–51]. These research papers show that the stiffnesses of shafts, bearings and gear teeth can directly affect the modal behaviour and dynamic response of geared rotors. Numerous linear and nonlinear dynamic analyses have been undertaken to understand the time-varying mesh stiffness effect on the dynamic behaviour of a gear pair since the gear mesh stiffness fluctuates during a contact period in reality [52–55]. A few parameter studies have investigated the constant gear mesh stiffness effect on the dynamic behaviour of planetary gearboxes and geared rotor systems, which is a valid assumption for heavily loaded gears [53]. Chen et al. [42] investigated the mesh stiffness effect on the critical speeds of a double-helical gear transmission system and highlighted the importance of the frequency veering phenomenon. It is shown that both gear mesh stiffness and gyroscopic effects can change the critical speeds in geared rotors at higher operating speeds. Rao et al. [41] showed a gear mesh stiffness region which affects the natural frequencies significantly in geared rotors. Parker and his colleagues [31,32] performed sensitivity analyses of the planetary gearbox vibration modes with regards to the gear mesh stiffness. The general support stiffness, normally provided by the bearings, is an important parameter to control vibration and modal parameters of a rotor systems, and has been demonstrated in many rotor dynamics books [56–60]. The support stiffness effect on the modal behaviour of geared rotors with flexible bearings [43] and with rigid bearings [45,46], and planetary gearboxes [31,32] has been studied in great detail. In planetary gearboxes, the effect of the radial support stiffness of the ring gears on the forced vibration response was presented by Li et al. [33]. It has been shown that bearings on the geared rotors have a considerable effect on the dynamic forces at the gear contacts and the natural frequencies of the system [43], and the gear mesh (contact) forces are approximately equal to the forces of stiff bearings in geared rotors [44]. The gear mesh stiffness is usually higher than other stiffness components in geared rotor systems, which makes it a significant parameter for higher vibration modes [47,48]. It is worth stating that lower modes (modes with lower natural frequency) can be controlled with bearing stiffnesses, and higher modes (modes with higher natural frequency) can be controlled with mesh stiffnesses in geared rotor systems.

Planetary gearboxes are commonly designed and manufactured with equally spaced planet gears. However, there can sometimes be positioning errors between the planet gears due to unequally spaced planets, which breaks the cyclic symmetry of the planetary gearbox structure. This phenomenon is known as planet mistuning in the literature, where there are some studies related to this phenomenon. For instance, the vibration mode sensitivity of planetary gears [32] and general compound planetary gears [31] to planet mistuning, and the modal behaviour of mistuned planetary gears [34] were investigated to identify the mistuning effect. In some of these sensitivity analyses [31,32], it has also been shown that natural frequencies of planetary gearboxes can be controlled easily by changing their mass and inertia parameters. Different numbers of planet gears are employed in planetary gearbox applications, normally ranging from three to seven. Eritenel and Parker performed modal analyses with their dynamic model for four and five planet gears, and they showed modal properties for the lowest ten vibration modes in their paper [23]. There is no detailed survey available how different numbers of planet gears affect the modal behaviour of planetary geared rotors. All of these studies considered the plan-

etary gearbox only and did not extend to the modal behaviour of planetary geared rotors to which these gearboxes are attached.

Although there are some parameter studies available for planetary geared rotors, they normally focus on particular aspect of the planetary gearbox parameter effects on the dynamics of planetary geared rotors, limiting the understanding to individual problems [50,61–64]. For example, a simple model (low fidelity) of the planetary gearbox, was used for the overall mass and stiffness parametric studies in reference [62], whereas a detailed three-dimensional model (high fidelity) of the planetary gearbox was used for modal behaviour identification in reference [63]. The simple model which assumes that planetary gearboxes consist of a certain distribution of mass/inertia and stiffness can capture the overall mass and stiffness parameters effect on the modal behaviour. However, it may not be sufficient to estimate the effect of the planetary gearbox parameters, such as gear contact and planet gear parameters, on the global modal behaviour, since the simple model does not include gear parameters such as helix angle, pressure angle, gear mesh stiffness, in their formulation. Therefore, a detailed planetary gearbox model for understanding the planetary gearbox parameter effects such as gear contact and planet gear parameters is needed.

When considering planetary gearboxes in a rotor dynamic system, two main aspects are of interest; their global effects on the overall dynamic behaviour of the geared rotor system, where mainly their mass, inertia and stiffness play a role, and their potential as an excitation source due to gear meshing action. This research paper investigates the modal sensitivity of the planetary geared rotor systems to the planet gear parameters, which has not been addressed systematically in the literature so far. The main motivation of this research is to provide a detailed understanding of how a variety of planet gear parameters affect the modal behaviour and global dynamics of planetary geared rotor systems, highlighting its novelty in terms of planetary geared rotor design. The focus of this research is on the global effect, rather than the internal planetary gearbox dynamics and potential excitation source, since the latter has been presented in great detail [65], while an in depth understanding of the former is still lacking. For this purpose, a three-dimensional hybrid dynamic model of a planetary geared rotor system is employed from reference [63], where the planetary gearbox and rotor system were modelled using the lumped parameter and finite element methods, respectively. In order to investigate rotor dynamics in the design space of planetary gearboxes, and the significant uncertainty surrounding the input parameters for the planetary gearbox, an extensive parameter study is then conducted to identify the sensitive planet gear parameters and highlight their impact on the modal behaviour of planetary geared rotors. Sensitivity of natural frequencies and vibration modes to the planet gear parameters is determined by computing the frequency shifts and comparing the mode shapes between the two extreme cases.

2. Dynamic modelling and analysis method

2.1. Dynamic model

A typical planetary geared rotor system consists of input and output shafts, several bearings, and a planetary gearbox, as seen in Fig. 1a. In planetary geared rotor systems, the main duty of the planetary gearbox is to couple the input and output shafts, reduce or increase the speed ratio between the two shafts, and increase or reduce the torque in the output shaft.

For the dynamic modelling in this research paper, a linear three-dimensional hybrid dynamic model of a planetary geared rotor system, including lateral, axial and torsional motions, is used from reference [63]. Robustness in global rotor dynamic response and fast computation features make this dynamic model more innovative compared to the full FE models. In summary, the hybrid dynamic model of a planetary geared rotor system is created using a combination of lumped parameter and finite element methods to model the planetary gearbox and rotor system, respectively, as seen in Fig. 1. All gear teeth contacts (gear meshes) and gearbox bearings are assumed to be flexible in the lumped parameter model of the planetary gearbox, whereas the planetary gearbox members, which are the ring gear, carrier, planet gears and sun gear, are assumed to be rigid. Flexibility of gear meshes is represented by linear springs acting on the plane of action normal to the gear tooth surfaces. Time-varying components of gear mesh stiffnesses due to changes in the number of tooth pairs in contact are neglected. Averaged gear mesh stiffnesses are used for the gear teeth contacts. 1-D rotating Timoshenko beam elements are used to construct the finite element model of the shafts. Both shaft and gearbox bearing elements are assumed to be flexible and consist of linear uncoupled translational and rotational spring elements. Uncoupled translational and rotational springs for the bearing supports were chosen in the dynamic analysis of the geared rotor system, as is common in the literature [41–43,66–68], to avoid complex cross-coupling due to the bearings [56–60], which may overshadow the planet gear effects in the parameter analysis.

It is important to point out that the dynamic model of the planetary gearbox used in reference [63] is based on Kahraman's two papers [22,24], published in 1994 and 2013 respectively. In this study, the carrier is assumed to be fixed and a stationary coordinate system is used for the modal sensitivity analyses. By using the already identified energy equations for the rotor-bearing system and planetary gearbox in reference [63], the system equation of motions can be obtained using Lagrange's equations of the second kind and a finite element assembly procedure. Finally, the system equation of motion of the planetary geared rotor system is written for free vibrations as

$$\mathbf{M}\ddot{\boldsymbol{q}}(t) + \left[\mathbf{C} + \mathbf{G}\left(\Omega_h, \Omega_{\mathrm{pi}}\right)\right]\dot{\boldsymbol{q}}(t) + \mathbf{K}\boldsymbol{q}(t) = 0. \tag{1}$$

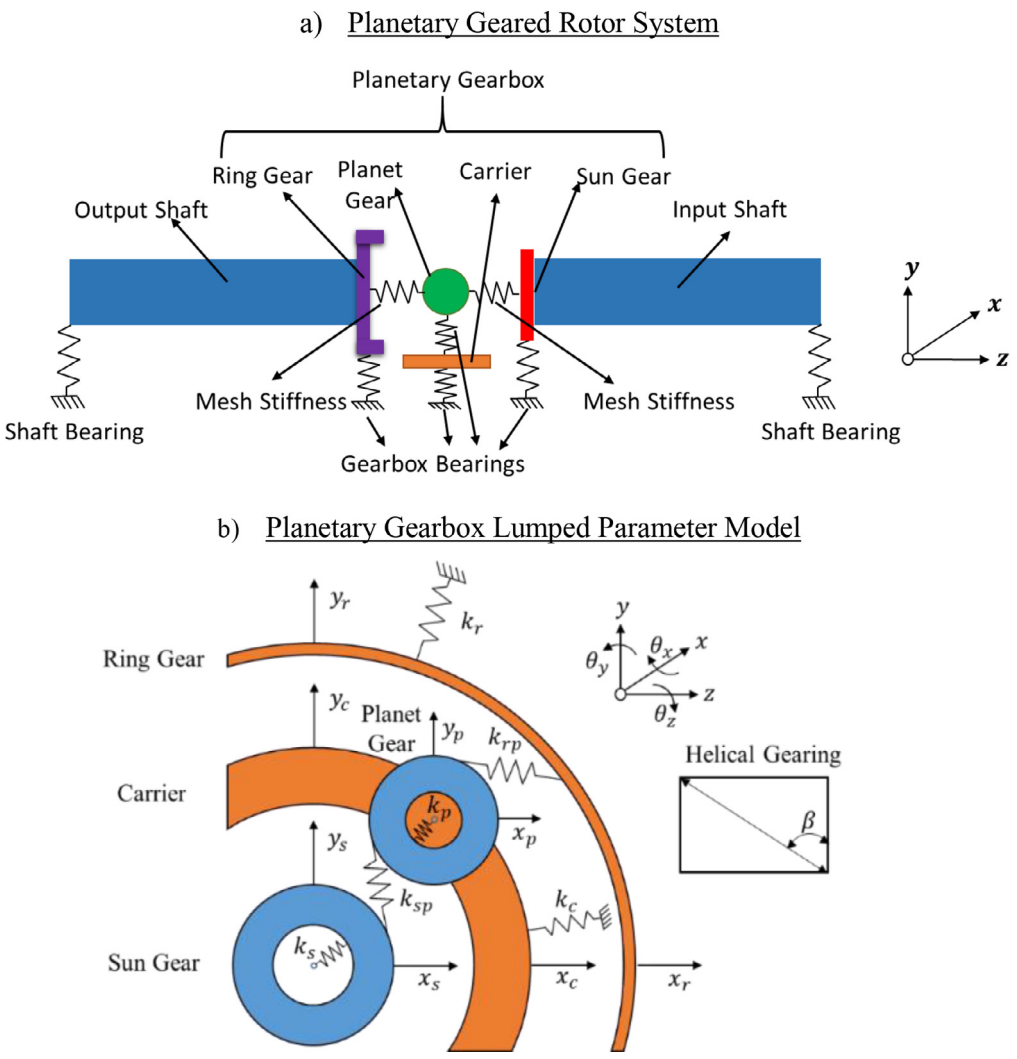

Fig. 1. Planetary geared rotor system and its elements, a) planetary geared rotor system, b) lumped parameter modelling of planetary gearbox [63].

where $\boldsymbol{q}$ is the vector of generalized coordinates, including lateral, torsional and axial motions, given by

$$\boldsymbol{q} = [q_s, q_g]. \tag{2}$$

Here, q_s and q_g represent the generalized coordinates of the input/output shafts and planetary gearbox, respectively. They are written as

$$\begin{aligned} \boldsymbol{q_s^i} &= \left[x_s^i, y_s^i, z_s^i, \theta_{xs}{}^i, \theta_{ys}{}^i, \theta_{zs}{}^i\right] \\ \boldsymbol{q_g^j} &= \left[x_g^j, y_g^j, z_g^j, \theta_{xg}{}^j, \theta_{yg}{}^j, \theta_{zg}{}^j\right] \end{aligned} \tag{3}$$

In Eq. (3), i is the index for input and output shafts (i = 1:2) respectively, and j is the planetary gearbox index (j = r,c,s,p1,…..,pN) for the ring gear (r), carrier (c), sun (s) and planet gears (p = p1,p2…..pN). In Eq. (1), **M, C, G, K** represent global system mass, damping, gyroscopic and stiffness matrices, which are explicitly written as

$$\begin{aligned} [\mathbf{M}] &= \mathbf{M}(\mathbf{M_s}, \ \mathbf{M_g}), \\ [\mathbf{G}] &= \mathbf{G}(\mathbf{G_s}, \ \mathbf{G_g}), \\ [\mathbf{K}] &= \mathbf{K}(\mathbf{K_s}, \mathbf{K_b}, \ \mathbf{K_g}), \\ [\mathbf{C}] &= \mathbf{C}(\mathbf{C_s}, \mathbf{C_b}, \mathbf{C_g}). \end{aligned} \tag{4}$$

In Eq. (4), subscripts which are s, g, b represent shaft (s), gearbox (g) and bearing (b). Details of the dynamic modelling of planetary geared rotor systems are provided in reference [63].

2.2. Modal analysis

The main modal parameters of the planetary geared rotor system, which are natural frequencies and mode shapes, can be computed numerically by solving the eigenvalue problem. The system equation of motion given in Eq. (1) can be rewritten as

$$\ddot{\boldsymbol{q}}(t) + \mathbf{M}^{-1}\left[\mathbf{C} + \mathbf{G}\left(\Omega_h, \Omega_{\mathrm{pi}}\right)\right]\dot{\boldsymbol{q}}(t) + \left(\mathbf{M}^{-1}\mathbf{K}\right)\boldsymbol{q}(t) = 0. \tag{5}$$

with the inverse matrix operation [69]. Then, the state space representation of the dynamic model in matrix form is obtained as

$$\begin{Bmatrix} \dot{\boldsymbol{q}} \\ \ddot{\boldsymbol{q}} \end{Bmatrix} = \begin{bmatrix} 0 & \boldsymbol{I} \\ -\mathbf{M}^{-1}\mathbf{K} & -\mathbf{M}^{-1}[\mathbf{C}+\mathbf{G}] \end{bmatrix} \begin{Bmatrix} \boldsymbol{q} \\ \dot{\boldsymbol{q}} \end{Bmatrix}. \tag{6}$$

where $\boldsymbol{I}$ is the identity matrix. Eq. (6) can be rewritten as

$$\{\dot{\boldsymbol{x}}\}_{2n\ \times 1} = [\mathbf{J}]_{2n\ \times\ 2n}\{\boldsymbol{x}\}_{2n\ \times 1} \tag{7}$$

which is the matrix equation for the standard eigenvalue problem. In Eq. (7), $\boldsymbol{x}$ is the state vector, and $\mathbf{J}$ is the Jacobian matrix. After solving the standard eigenvalue problem, the eigenvalue $[\lambda]$ and eigenvector $[\phi]$ matrices can be computed, and the natural frequencies and mode shapes obtained. For the mode shape comparison between different cases in the parameter study, the Modal Assurance Criteria (MAC) is employed, which is defined as [70]

$$MAC(A,B)_{(i,j)} = \frac{\left|\{\phi_A\}_i^T\{\phi_B\}_j\right|^2}{\left(\{\phi_A\}_i^T\{\phi_A\}_i\right)\left(\{\phi_B\}_j^T\{\phi_B\}_j\right)} \tag{8}$$

where ϕ_A and ϕ_B represent the eigenvectors of the two cases. i and j are indices for the corresponding mode number.

To quantify the modal sensitivity, frequency shifts between the two extreme cases are calculated as

$$\text{frequency shift } (\%) = \frac{\left|\omega_i - \omega_f\right|}{\omega_i} \times 100 \tag{9}$$

where ω_i and ω_f represent the initial (baseline) and final (updated) natural frequencies.

Modal energy analysis is also used for the coupling level quantification between the gearbox and rotor system. The modal energy percentage of the gearbox is written as

$$\varepsilon = \frac{L_r^g}{L_r} \times 100. \tag{10}$$

Here, L_r^g and L_r represent total energies of the gearbox and whole rotor system. They can be written as

$$L_r = T_r + V_r$$

$$L_r^g = T_r^g + V_r^g \tag{11}$$

where T and V are the kinetic and potential energies. Full derivation of the modal energy analysis is available in reference [63].

The modal analyses throughout this study are carried out in "GEAROT" [62] rotor dynamics software, where the standard eigenvalue solution is used because of its computational performance [69,71]. It should be noted that all damping in the planetary geared rotor system is neglected. Although gyroscopic effects of the whole planetary gearbox were previously studied in reference [63], gyroscopic effects of the planet gears are specifically investigated in this paper. The baseline system parameters of the hybrid dynamic model are imported from reference [63] for this study, and are provided in Table 1. For this system, maximum speed and speed ratio were specified as 8000 rpm and 3.04, respectively in reference [63]. The specifications represent the expected higher power requirements of a geared turbofan, although the numbers used are purely academic. The maximum torque of this system has been approximately computed as 30 kNm by taking into account the torsional shear stresses.

3. Modal sensitivity to planet gear parameters

To provide a better understanding how the planet gear parameters affect dynamics of the planetary geared rotor systems, a comprehensive modal sensitivity analysis is presented in this section. The modal sensitivity analysis mainly shows the planet gear parameters effects on the natural frequencies and mode shapes. The parameter study includes the effect of number of planet gears, planet mistuning, gear mesh stiffness, planet gear mass and planet gear speed. Gyroscopic effects of the planetary geared rotor system are only considered in the parameter study of planet gear speed (Section 3.5).

Table 1
Baseline system parameters of the planetary geared rotor system [63].

Parameter	Output Shaft	Input Shaft	Carrier	Ring	Planets	Sun	Ring-Planet	Sun- Planet
Length [m]	2	2						
Width [m]			0.02	0.1	0.1	0.1		
Outer Diameter [m]	0.2	0.2	0.63	0.7	0.2	0.23		
Inner Diameter [m]			0.23	0.63	0.18	0.2		
Material density [kg/m^3]	7800	7800	7800	7800	7800	7800		
Young's modulus [GPa]	211	211						
Shear modulus [GPa]	81.2	81.2						
Bearing radial stiffness [N/m]	10^9	10^9	10^9	10^9	10^9	10^9		
Bearing axial stiffness [N/m]	10^9	10^9	10^9	10^9	10^9	10^9		
Bearing tilting stiffness [N.m/rad]	10^7	10^7	10^7	10^7	10^7	10^7		
Bearing torsional stiffness [N.m/rad]	0	0	10^{11}	0	0	0		
Helix angle β [deg]				30	30	30		
Transverse pressure angle ϕ [deg]				22.5	22.5	22.5		
Mesh Stiffness [N/m]							10^8	10^8
Number of planets					4			
Number of beam elements	18	18						
Total degree of freedom	114	114	6	6	24	6		

3.1. Number of planet gears

In the parameter study of number of planet gears, three cases were considered, namely helical planetary geared rotors with three, four (baseline), five planets. The results of the modal analyses are given in Table 2. It must be noted that the other gear parameters for the planets were not changed, leading to an increased total mass of the planets and more total gear contacts, and hence higher stiffness, for the five-planet gear configuration.

The resulting mode shapes of the helical planetary geared rotors with three, four and five planets for the first 25 modes are given in Figs. A1, A2 and A3 in the Appendix, where rigid body torsional, lateral and coupled torsional-axial modes can be clearly seen. In changing from three planets to five planets, the natural frequencies of the torsional-axial modes tend to increase due to the fact that the added gear mesh stiffness in the system overshadows the added inertia of the two planets. The exception here is 20th mode of the three-planet gear system, where a significant drop in frequency from 622 Hz to 573 Hz is observed. This is mainly because of the higher gearbox modal energy at the 20th mode as presented in Table 2, which highlights the local dynamic behaviour rather than the global dynamic behaviour. Basically, most of the modal energy is stored in the gearbox and there is nearly no shaft activity in this mode. On the other hand, the natural frequencies of the lateral modes tend to decrease with respect to the number of planets, except for the first four lateral modes which remain constant. This behaviour is observed because the gearbox is located at the nodal point and has less modal energy in these lateral modes. Overall, it is important to point out that the modes which have higher gearbox modal energy are more sensitive to the frequency shifts with respect to the number of planet gears.

The mode shapes of the helical planetary geared rotors with three and five planets were compared using the Modal Assurance Criteria, as seen in Fig. 2. Generally, there is a reasonably good mode shape agreement between the two configurations, although the order of the modes is significantly affected by the presence of different planet gear numbers. This reordering is partially due to the presence of repeated modes and partially due to the mode veering. In some cases, lower mode shape agreement is observed due to the mode shape distortions between the two configurations. Overall, there is a good mode shape agreement except for some distorted mode shapes when mode veering is taken into account.

In general, the first five modes of the spur and helical planetary geared rotors are found to be insensitive to the parameters. This is due to the choice of system parameters. If rigid shorter shafts or more compliant gears were used, it would be expected that the first five modes would be more sensitive to the system parameters. Increasing the number of planet gears leads to an increase in the natural frequencies of the torsional-axial modes, whereas this leading to a decrease in the natural frequencies of the lateral modes in general. Thus, a planetary gearbox behaves more rigidly in torsional-axial vibrations and more flexibly in lateral vibrations with the increase in the number of planet gears. From the modal behaviour perspective, it could be suggested that different numbers of planet gears can be used in order to control the natural frequencies of the torsional-axial modes and lateral modes. It should also be noted that there is a reverse effect between the torsional-axial modes and lateral modes in terms of flexibility with respect to the number of planet gears.

3.2. Planet mistuning

Planet mistuning is known as the positioning errors between the planet gears due to unequally spaced planets phenomenon. In this parameter study, the planet mistuning range was chosen from 0° (baseline) to 14° with only one planet

Table 2
First 30 modes for the helical planetary geared rotors with three, four and five planets.

Mode #	Three Planets			Four Planets (Baseline)			Five Planets		
	Natural Freq. [Hz]	Mode Type	Gearbox Modal Energy%	Natural Freq. [Hz]	Mode Type	Gearbox Modal Energy%	Natural Freq. [Hz]	Mode Type	Gearbox Modal Energy%
1	0	Torsional	26	0	Torsional	27	0	Torsional	28
2	114	Lateral	10	114	Lateral	10	114	Lateral	10
3	114	Lateral	10	114	Lateral	10	114	Lateral	10
4	115	Lateral	9	115	Lateral	10	115	Lateral	10
5	115	Lateral	9	115	Lateral	10	115	Lateral	10
6	197	Torsional - Axial	65	220	Torsional - Axial	60	237	Torsional - Axial	56
7	300	Torsional - Axial	30	301	Torsional - Axial	29	301	Torsional - Axial	30
8	316	Torsional - Axial	26	318	Torsional - Axial	27	305	Lateral	98
9	332	Lateral	16	322	Lateral	94	305	Lateral	98
10	332	Lateral	16	322	Lateral	94	322	Torsional - Axial	27
11	340	Lateral	48	333	Lateral	17	333	Lateral	16
12	340	Lateral	48	333	Lateral	17	333	Lateral	16
13	351	Lateral	62	346	Lateral	15	346	Lateral	12
14	351	Lateral	62	346	Lateral	15	346	Lateral	12
15	465	Torsional - Axial	17	466	Torsional - Axial	20	467	Torsional - Axial	22
16	509	Lateral	61	508	Lateral	62	507	Lateral	62
17	509	Lateral	61	508	Lateral	62	507	Lateral	62
18	602	Lateral	21	595	Torsional - Axial	97	573	Torsional - Axial	97
19	602	Lateral	21	601	Lateral	23	598	Lateral	27
20	622	Torsional - Axial	98	601	Lateral	23	598	Lateral	27
21	652	Lateral	29	649	Lateral	32	645	Lateral	34
22	652	Lateral	29	649	Lateral	32	645	Lateral	34
23	719	Lateral	91	710	Lateral	84	705	Lateral	77
24	719	Lateral	91	710	Lateral	84	705	Lateral	77
25	780	Torsional - Axial	16	782	Torsional - Axial	18	786	Torsional - Axial	20
26	873	Lateral	27	873	Lateral	28	874	Lateral	29
27	873	Lateral	27	873	Lateral	28	874	Lateral	29
28	942	Lateral	19	908	Gearbox	100	908	Gearbox	100
29	942	Lateral	19	943	Lateral	18	908	Gearbox	100
30	1026	Torsional - Axial	85	943	Lateral	18	945	Lateral	18

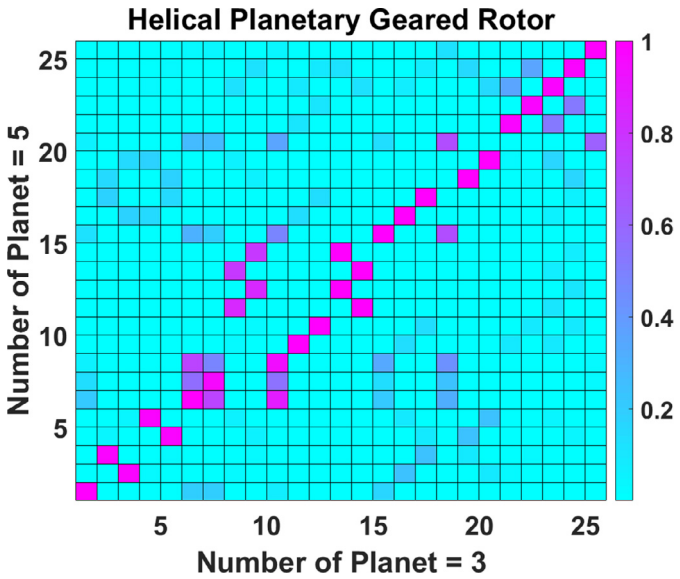

Fig. 2. MAC comparison for the modes of helical planetary geared rotors with three and five planets.

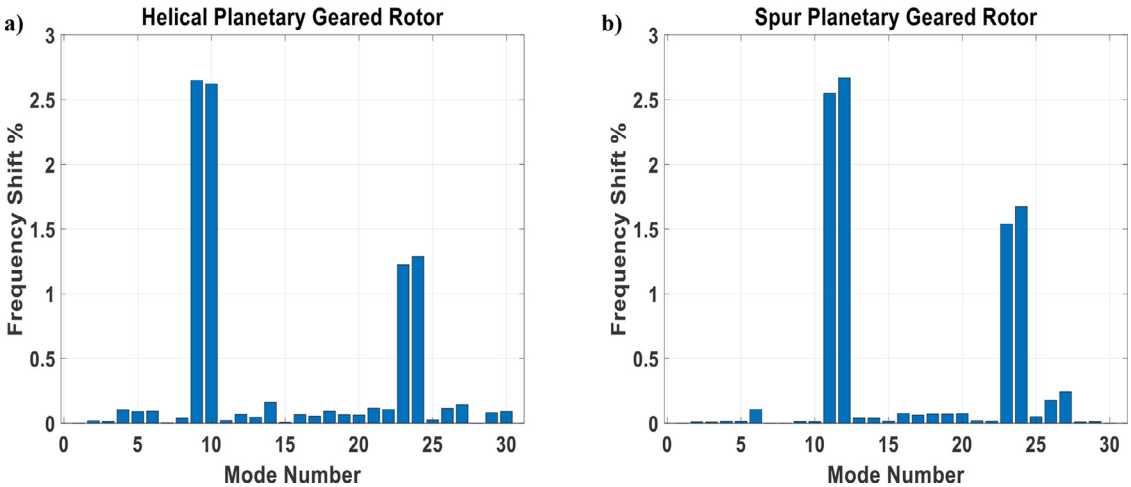

Fig. 3. Frequency shifts of planetary geared rotor vibration modes due to planet mistuning, a) helical, b) spur.

in the assembly being re-located. Here, 14° for the mistuning is considered as an extreme case. The frequency shifts were computed for the helical and spur planetary geared rotors and are shown in Fig. 3.

Natural frequency sensitivity of the helical and spur planetary geared rotors to planet mistuning for the 6th to 25th modes are shown in Fig. 4. Fig. 3 shows that there is no significant change in the natural frequencies due to planet mistuning with all changes below 3% for the helical and spur gear configurations. The modes with more than a 1% frequency shift were investigated further to identify the sensitive modes.

In the helical planetary geared rotor, significant frequency shifts occur for the 9th and 10th modes at 2.6%, for the 23rd mode at 1.2%, and for the 24th mode at 1.3%. It should be noted that these modes are originally lateral if there is no planet mistuning. The torsional-axial modes are found to be barely affected by mistuning compared to the lateral modes, and the changes were less than 1%. For the spur planetary geared rotor, the significant frequency shifts are seen for the 11th and 12th gearbox modes at 2.5% and 2.7% respectively, and for the 23rd and 24th lateral modes at 1.5% and 1.7%, respectively. In the spur planetary geared rotor, it is found that the axial modes are not sensitive to mistuning because there is no geometric interaction of the mistuning in the axial direction. Furthermore, the torsional modes are barely affected compared to the lateral modes.

Due to the breaking cyclic symmetry of the planetary gearbox structure, the planet mistuning results in lateral-torsional-axial coupling in helical planetary geared rotors and lateral-torsional coupling in spur planetary geared rotors. Mode shapes

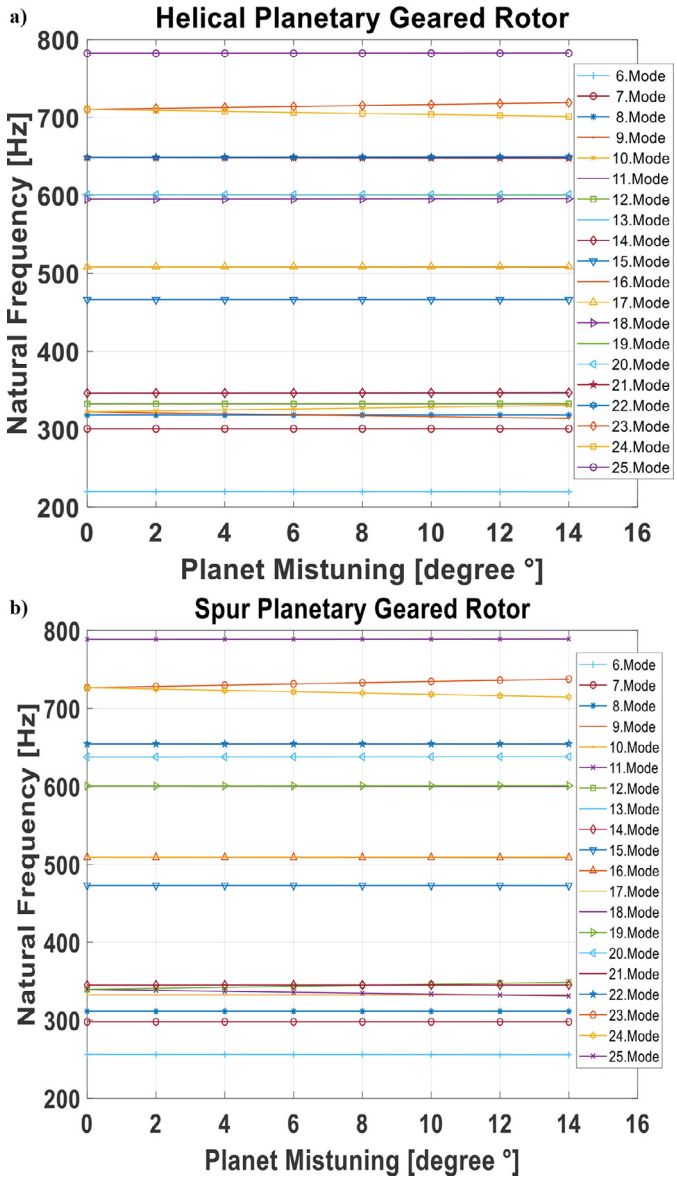

Fig. 4. Sensitivity of planetary geared rotor vibration modes to planet mistuning, a) helical, b) spur.

of the highest frequency shifting observed modes in the helical planetary geared rotor are given in Fig. 5, and show the coupled lateral-torsional-axial modes due to the planet mistuning effect. As a result, modes of the mistuned helical planetary geared rotors are coupled in the lateral, torsional and axial directions. Depending on the vibration mode sensitivity levels, the coupled lateral-torsional-axial modes can be clearly detected in their mode shapes.

The natural frequency shifts due to planet mistuning were negligible in both helical and spur planetary geared rotors while it can directly affect their mode shapes. Mistuning can lead to an increase or decrease in the natural frequencies of the planetary geared rotors.

The mode shapes for the tuned and mistuned cases were compared with the MAC matrices for the helical and spur planetary geared rotors in Fig. 6. For the helical planetary geared rotor, there is nearly 100% mode shape agreement for the torsional rigid body, torsional-axial and gearbox modes. In contrast, there is a reduced MAC agreement for the lateral modes of the tuned system because of the occurrence of lateral-torsional-axial coupling for these modes in the mistuned case. For the spur planetary geared rotor, a good mode shape agreement can be observed for all torsional and axial modes and some of the gearbox modes. Lower mode shape agreements are observed for the lateral modes of the tuned system due to the lateral-torsional coupling in the mistuned one.

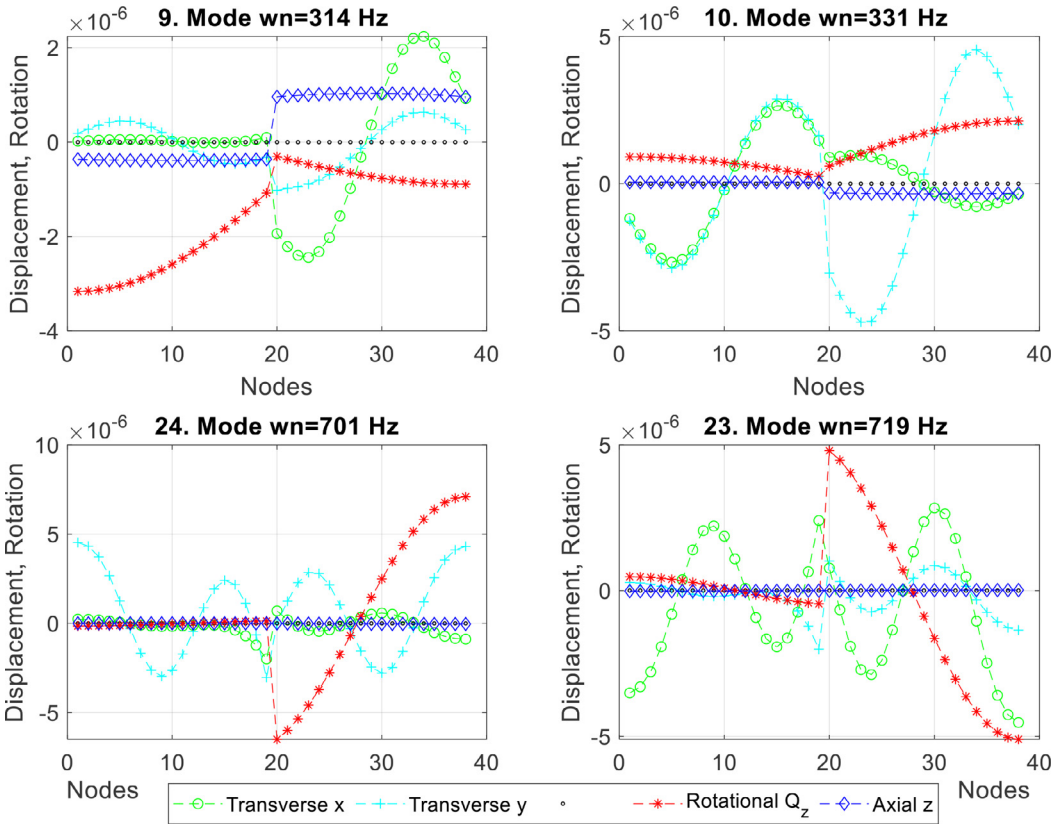

Fig. 5. Coupled lateral-torsional-axial vibration modes of the helical planetary geared rotor with unequally spaced planets.

In summary, planet gear mistuning appears to have a relatively small effect on the natural frequencies of the geared rotor system, but it introduces lateral-torsional-axial coupling in the case of helical gearboxes and lateral-torsional coupling in the case of spur planetary gearboxes due to breaking cyclic symmetry. Original lateral modes in the tuned system are also found to be more sensitive to the planet mistuning. It is important to point out that unexpected axial vibrations can lead to lateral vibrations in the mistuned helical planetary geared rotor systems due to the coupled lateral-torsional-axial modes. For instance, the axial thrust forces in geared turbofan engines may excite their lateral modes and vice versa.

3.3. Gear mesh stiffness

The gear mesh stiffness is defined as the contact stiffness between the engaging gear teeth, which includes the bending stiffness, axial compressive stiffness, shear stiffness, Hertzian contact stiffness and fillet foundation stiffness [72,73]. It is known that gear mesh stiffness is a function of several parameters such as gear tooth geometry, gear tooth profile, gear material properties, transverse pressure angle, transmitted load, position of contact etc. [73–75]. There are different approaches to calculate gear mesh stiffness accurately in the literature such as analytical, finite element and hybrid analytical-finite element methods [76,77]. The gear mesh stiffness fluctuates during the gear contact period [52,53]. In order to perform time-invariant modal analysis, the gear mesh stiffness is first obtained using the analytical method [72]. Subsequently, constant gear mesh stiffness is computed by averaging the stiffness, which is known as the averaged gear mesh stiffness. This parameter study investigates the effect of the averaged gear mesh stiffness of spur and helical gears on a large range of vibration modes of the presented planetary geared rotor systems.

A gear mesh stiffness range between 10^8 N/m and 10^9 N/m (i.e. a factor of 10) was selected for the parameter study on the basis of reference [22–24]. The first 30 modes and frequency shifts between the extreme 10^8 N/m and 10^9 N/m gear mesh stiffness values were computed for both the helical and spur planetary geared rotors, as shown in Table 3, where the corresponding mode types are also given. It should be noted that $k_m = 10^8$ [N/m] is the baseline gear mesh stiffness, as given in Table 1. The gear mesh stiffness effect on the natural frequencies is shown for the significant modes in Fig. 7. Not surprisingly, the natural frequencies of the geared rotor system increase with increasing mesh stiffness. There is no significant change in the natural frequencies up to the 6th mode, thus the first five modes were not plotted. To understand the reason

Table 3
Vibration modes of the helical and spur planetary geared rotors for two gear mesh stiffnesses.

Helical Planetary Geared Rotor					Spur Planetary Geared Rotor			
Mode #	$k_m = 10^8$ [N/m] (Baseline) Nat. Freq. [Hz]	$k_m = 10^9$ [N/m] Nat. Freq. [Hz]	Mode Type	Freq. Shift%	$k_m = 10^8$ [N/m] (Baseline) Nat. Freq. [Hz]	$k_m = 10^9$ [N/m] Nat. Freq. [Hz]	Mode Type	Freq. Shift%
1	0	0	Torsional	0	0	0	Torsional	0
2	114	114	Lateral	0	113	113	Lateral	0
3	114	114	Lateral	0	113	113	Lateral	0
4	115	117	Lateral	1	114	115	Lateral	0
5	115	117	Lateral	1	114	115	Lateral	0
6	220	283	Torsional - Axial	29	256	369	Torsional	44
7	301	305	Torsional - Axial	1	298	298	Axial	0
8	318	373	Torsional - Axial	17	311	311	Axial	0
9	322	328	Lateral	2	333	334	Lateral	0
10	322	328	Lateral	2	333	334	Lateral	0
11	333	335	Lateral	1	340	340	Gearbox	0
12	333	335	Lateral	1	340	340	Gearbox	0
13	346	352	Lateral	2	345	347	Lateral	1
14	346	352	Lateral	2	345	347	Lateral	1
15	466	522	Torsional - Axial	12	473	540	Torsional	14
16	508	514	Lateral	1	509	514	Lateral	1
17	508	514	Lateral	1	509	514	Lateral	1
18	595	614	Torsional - Axial	3	601	602	Lateral	0
19	601	602	Lateral	0	601	602	Lateral	0
20	601	602	Lateral	0	638	638	Gearbox	0
21	649	651	Lateral	0	655	655	Lateral	0
22	649	651	Lateral	0	655	655	Lateral	0
23	710	825	Lateral	16	727	834	Lateral	15
24	710	825	Lateral	16	727	834	Lateral	15
25	782	879	Torsional - Axial	12	789	918	Torsional	16
26	873	929	Lateral	6	880	946	Lateral	8
27	873	929	Lateral	6	880	946	Lateral	8
28	908	1783	Gearbox	96	948	1061	Lateral	12
29	943	1035	Lateral	10	948	1061	Lateral	12
30	943	1035	Lateral	10	1077	2119	Gearbox	97

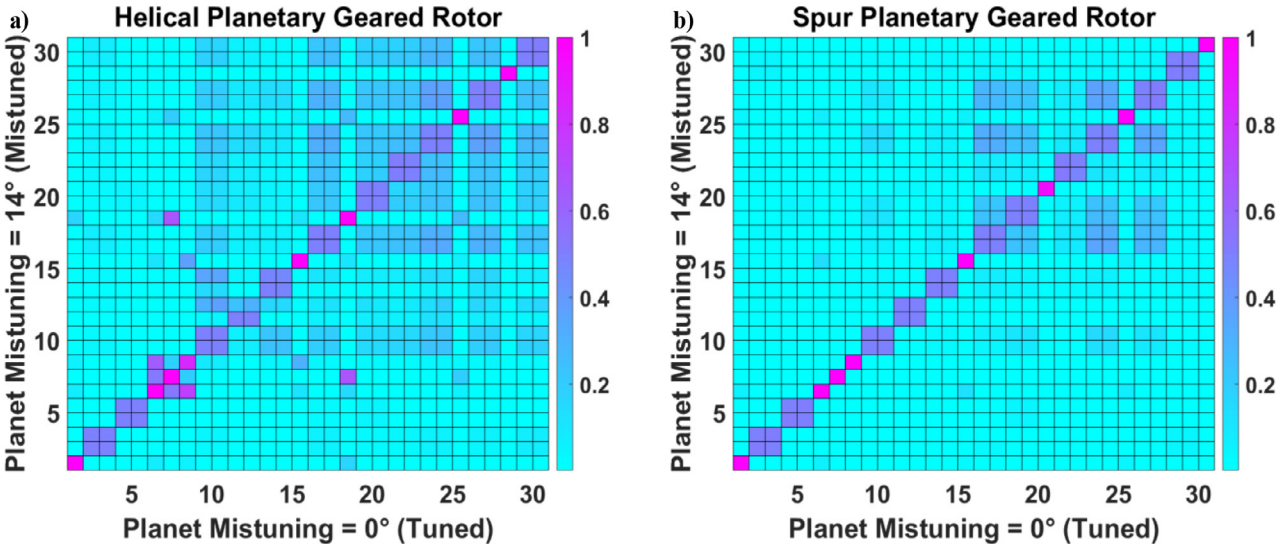

Fig. 6. MAC for modes with planet mistuning, a) helical, b) spur.

for the vibration mode sensitivity, the modes which have more than 10% frequency shift were investigated further. For the helical planetary geared rotor, the highest frequency shifts were computed as 29%, 17%, 12% and 12% for the 6th, 8th, 15th and 25th torsional-axial modes, respectively. Similarly, the frequency shifts were computed as 16% for the 23rd and 24th lateral modes and 96% for the 28th gearbox mode, as given in Table 3. In general, the torsional-axial modes in the helical planetary geared rotors are much more sensitive to the gear mesh stiffness change compared to the lateral modes. The gearbox modes are directly affected by the gear mesh stiffness change as clearly seen for the gearbox mode (28th mode). For the spur planetary geared rotor, the highest frequency shifts were computed as 44%, 14% and 16% for the 6th, 15th and 25th torsional modes, respectively. Moreover, the frequency shifts for the 23rd, 24th, 28th and 29th lateral modes were computed as 15%, 15%, 12% and 12%, respectively, and 97% for the 30th mode (gearbox mode). All the torsional modes within the first 30 modes are found to be much more sensitive to the gear mesh stiffness change in the spur planetary geared rotor. The axial modes of the spur planetary geared rotor are not sensitive to the gear mesh stiffness change since there is no axial component of the gear mesh stiffness in spur gears.

When comparing the helical and spur planetary geared rotor modes, there are some torsional-axial modes in the helical planetary geared rotor, which are more sensitive to the gear mesh stiffness change due to the fact that the torsional deformation dominates the axial deformation for these modes. This can be directly inferred from the torsional and axial modes of the spur planetary geared rotor given in Table 3.

The MAC matrices between the modes for the 10^8 N/m and 10^9 N/m gear mesh stiffness values are shown in Fig. 8. They further highlight the dependence of the mode shapes of the helical and spur planetary geared rotors on the gear mesh stiffness. For the helical planetary geared rotor, there is little change in the mode shapes up to the 26th mode and at the 28th mode. For the spur planetary geared rotor, a good mode shape agreement up to the 30th mode is also seen except the 26th, 27th, 28th and 29th modes due to the mode veering phenomenon for these modes, leading to unmatched cases in the MAC plot. The reduced MAC agreement seen at the higher modes (modes with higher natural frequency) for both the helical and spur planetary geared rotors, indicates that a change in gear mesh stiffness couples the higher global modes of a planetary geared rotor system.

Briefly, the torsional-axial modes of helical planetary geared rotors and the torsional modes of spur planetary geared rotors are more sensitive to gear mesh stiffness than their lateral modes. For the gear mesh stiffness, the dominance of the torsional components in the torsional-axial modes of helical planetary geared rotors determine the vibration mode sensitivity level, because the axial modes in spur planetary geared rotors are not affected by these contact parameters. As a result, the torsional modes are sensitive to gear mesh stiffness. Gear mesh stiffness is more influential at the higher lateral modes when looking at the frequency shifts and mode shape comparisons for these modes. Natural frequencies of planetary geared rotor systems increase with respect to the gear mesh stiffness.

3.4. Planet gear mass

The mass and inertia of gearboxes directly change with respect to gear material density. By considering this effect, a parameter study for different planet gear material densities of the spur and helical planetary geared rotors is presented. Aluminium, cast iron, bronze, steel and plastic are the commonly used gear materials in gearboxes [78,79]. amongst these material, nylon plastic gears have the lowest density at 1150 kg/m^3 and steel gears have the highest density at 7800 kg/m^3.

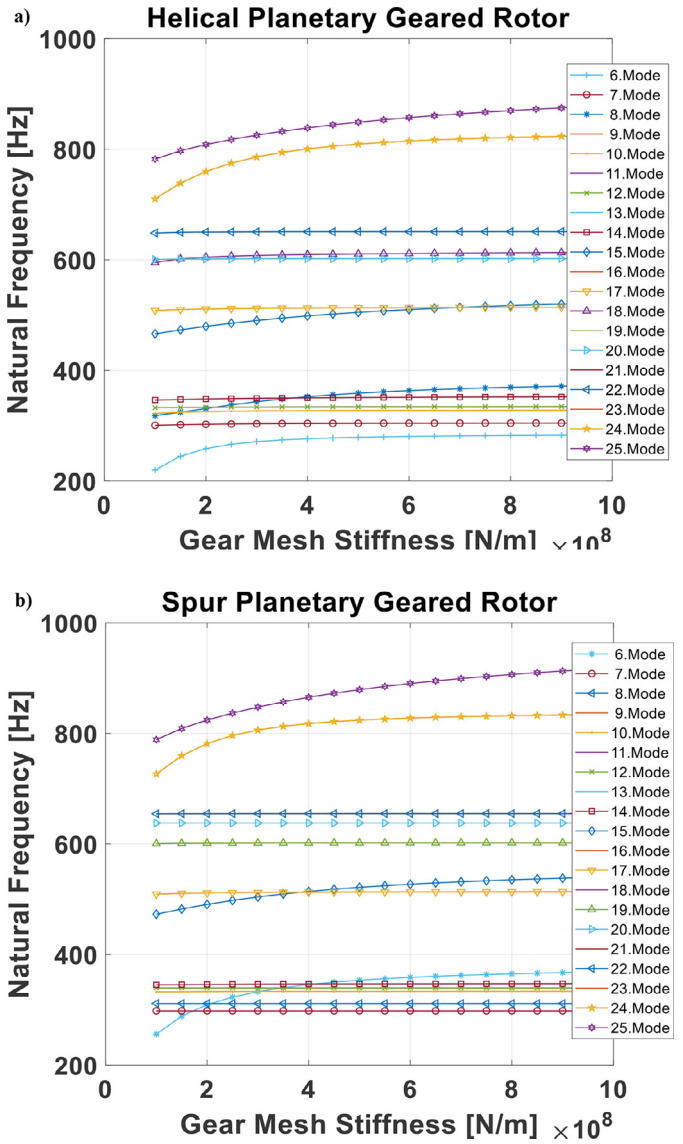

Fig. 7. Sensitivity of the planetary geared rotor vibration modes to gear mesh stiffness, a) helical, b) spur.

Therefore, a gear material density range from 1150 kg/m^3 to 7800 kg/m^3 was selected for an extensive parameter study. It should be noted that gear mesh stiffness and other system parameters were assumed to be constant while changing gear material density. Material of the shafts was also unchanged. After the modal analysis was performed, the frequency shifts between the two extreme cases, which are 1150 kg/m^3 and 7800 kg/m^3, were computed for the first 25 modes, as shown in Table 4. Frequency variations up to 30% were observed for both helical and spur gear configurations.

The gear material density of 7800 kg/m^3 is the baseline for the analysis of the vibration modes for both helical and spur planetary geared rotors (see Table 1). The gear material density effect on the natural frequencies is shown in Fig. 9 for the significant modes (more than 15% frequency shift) between the 6th and 25th modes since there is no significant change in the natural frequencies up to the 6th mode. In the helical planetary geared rotor, the important frequency shifts are for the 13th and 14th lateral modes at 28%, and for the 18th torsional-axial mode at 25% respectively. Moreover, the 23rd and 24th lateral modes show remarkable frequency shift at 16%. It is important to point out that there is a mode veering between the 13th and 14th mode family and the 9th and 10th mode family. Therefore, there can be an energy exchange between these mode families. In the spur planetary geared rotor, the highest frequency shifts are seen for the 11th, 12th and 20th gearbox modes. Furthermore, the 23rd and 24th lateral modes show remarkable frequency shift at 15%, similar to the lateral modes in the helical planetary geared rotor. On the other hand, the axial modes of the spur planetary geared rotor are not sensitive to the density change due to the higher rigidity of the rotor system in the axial direction. Overall, the gearbox modes are

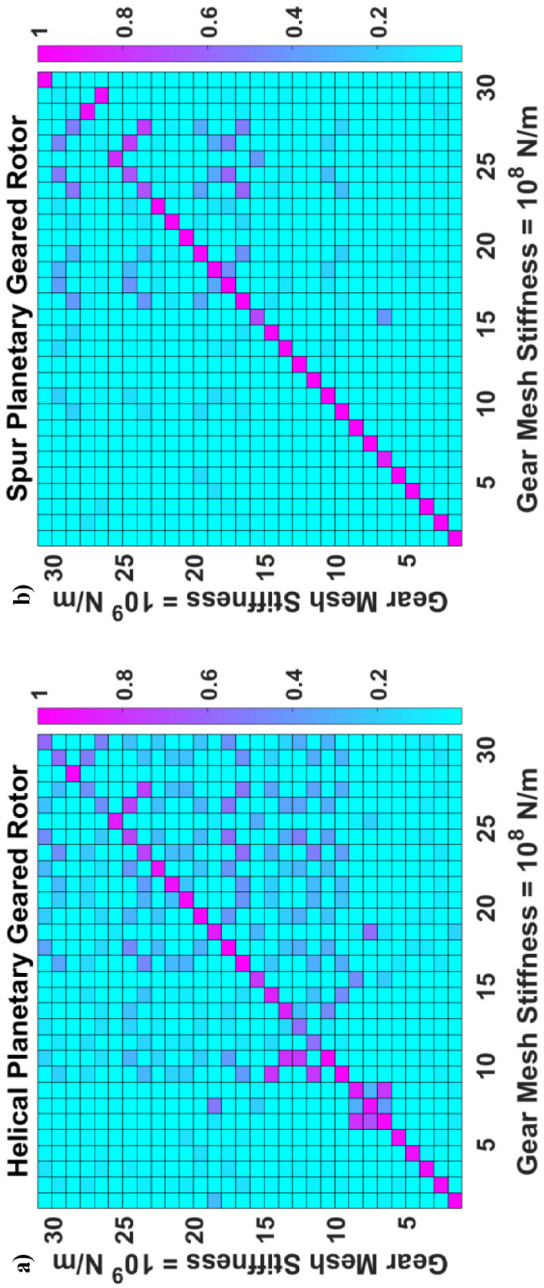

Fig. 8. MAC for modes with 10^8 and 10^9 N/m gear mesh stiffness, a) helical, b) spur.

Table 4
Vibration modes of the helical and spur planetary geared rotors for two gear material densities of the planetary gearbox.

Helical Planetary Geared Rotor					Spur Planetary Geared Rotor			
Mode #	ρ_p = 1150 kg/m^3 Nat. Freq. [Hz]	ρ_p = 7800 kg/m^3 (Baseline) Nat. Freq. [Hz]	Mode Type	Freq. Shift%	ρ_p = 1150 kg/m^3 Nat. Freq. [Hz]	ρ_p = 7800 kg/m^3 (Baseline) Nat. Freq. [Hz]	Mode Type	Freq. Shift%
1	0	0	Torsional	0	0	0	Torsional	0
2	114	114	Lateral	0	113	113	Lateral	0
3	114	114	Lateral	0	113	113	Lateral	0
4	115	115	Lateral	0	114	114	Lateral	0
5	115	115	Lateral	0	114	114	Lateral	0
6	221	220	Torsional - Axial	1	258	256	Torsional	1
7	302	301	Torsional - Axial	0	298	298	Axial	0
8	318	318	Torsional - Axial	0	311	311	Axial	0
9	345	322	Lateral	7	333	333	Lateral	0
10	345	322	Lateral	7	333	333	Lateral	0
11	333	333	Lateral	0	441	340	Gearbox	30
12	333	333	Lateral	0	441	340	Gearbox	30
13	443	346	Lateral	28	345	345	Lateral	0
14	443	346	Lateral	28	345	345	Lateral	0
15	474	466	Torsional - Axial	2	480	473	Torsional	2
16	516	508	Lateral	1	515	509	Lateral	1
17	516	508	Lateral	1	515	509	Lateral	1
18	743	595	Torsional - Axial	25	607	601	Lateral	1
19	606	601	Lateral	1	607	601	Lateral	1
20	606	601	Lateral	1	751	638	Gearbox	18
21	658	649	Lateral	2	656	655	Lateral	0
22	658	649	Lateral	2	656	655	Lateral	0
23	824	710	Lateral	16	838	727	Lateral	15
24	824	710	Lateral	16	838	727	Lateral	15
25	800	782	Torsional - Axial	2	808	789	Torsional	2

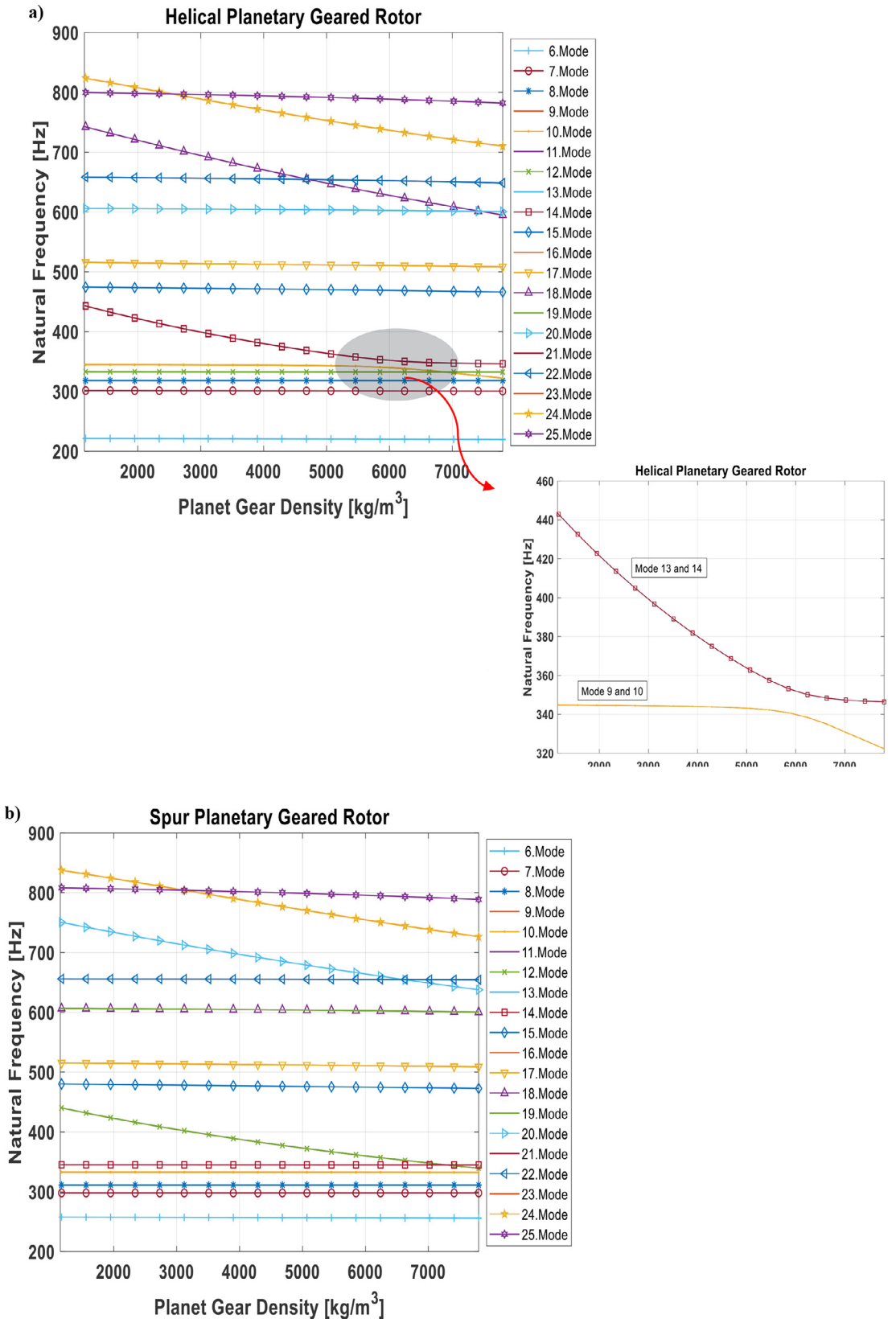

Fig. 9. Sensitivity of the planetary geared rotor vibration modes to gear material density, a) helical, b) spur.

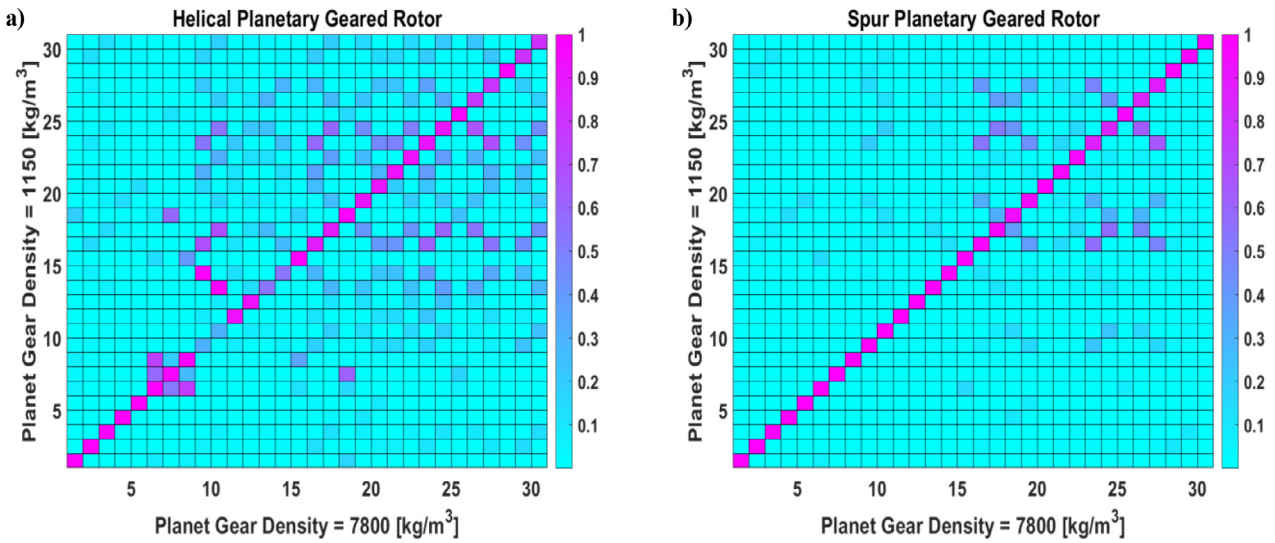

Fig. 10. MAC for modes with different gear material densities, a) helical, b) spur.

more sensitive to the planet gear material density change compared to the other modes in planetary geared rotors. Another important observation is that the lateral modes are slightly more sensitive to the density change than the torsional and torsional-axial modes. Not surprisingly, the natural frequencies of both helical and spur planetary geared rotors decrease with increasing material density.

A comparison of the mode shapes between the two extreme cases for the gear material density (1150 kg/m^3 and 7800 kg/m^3) via the modal assurance criteria is shown in Fig. 10. There is a good mode shape agreement up to the 8th mode for the helical planetary geared rotor, however for higher modes (modes with higher natural frequency) the agreement is much poorer due to mode veering and the distortion between the modes. Overall, there is a good agreement when looking at the MAC for the spur planetary geared rotor. The gear density can have a significant impact on both the natural frequencies and the mode shapes of the geared rotor system, highlighting the importance of taking the correct material properties into account when conducting a rotor dynamic analysis.

When evaluating the gear mesh stiffness and planet gear mass parameters, the mode shapes of both spur and helical planetary geared rotors are not significantly affected by them. On the other hand, they can significantly affect their natural frequencies. Lateral vibration modes are found to be more sensitive to the gearbox mass compared with the other global modes (coupled torsional-axial, uncoupled torsional and uncoupled axial modes). It is found that the torsional and coupled torsional-axial modes are more sensitive to the gear mesh stiffness, whereas the lateral modes are more sensitive to the gear material density. As general advice, the torsional and torsional-axial modes can be controlled by changing the gear mesh stiffness, and the lateral modes can be controlled by changing the mass of the planet gears. The latter implies that shafts are stiffer than the planetary gearbox in terms of torsional and axial dynamics whereas they are softer than the planetary gearbox in terms of lateral dynamics. This means that the dynamic model of the planetary gearbox should be stiffer in the lateral directions and softer in the torsional and axial directions than the shaft dynamic model if a simple gearbox model is used.

3.5. Planet gear speed

Operating speed of the planetary geared rotors can affect the modal parameters due to the generation of gyroscopic moments. The so-called gyroscopic moments in this planetary geared rotor system can originate from the sun, ring, planet gears, carrier and input/output shafts. They can create lateral backward and forward whirling modes on the global rotor system.

In the previous study [63], gyroscopic effect of the whole planetary gearbox was investigated. In this study, to understand only the planet gear speed effect on the modal behaviour, three case studies have been created as presented in Table 5. They are **(a)** with gearbox gyroscopic effect (including gyroscopic effects of ring, sun and planet gears, carrier and shafts), **(b)** without gearbox gyroscopic effect (including gyroscopic effects of shafts) and **(c)** without planet gear gyroscopic effect (including gyroscopic effects of ring, and sun gears, carrier and shafts). For this purpose, Campbell diagrams were plotted for the five significant modes in Fig. 11, where it is clearly seen that main gyroscopic effect inside the planetary gearbox is produced by the planet gears for mode 9 (Lateral BW) and mode 10 (Lateral FW). On the other hand, gyroscopic moments generated by the shafts are more dominant at mode 11 (Lateral BW) and mode 12 (Lateral FW).

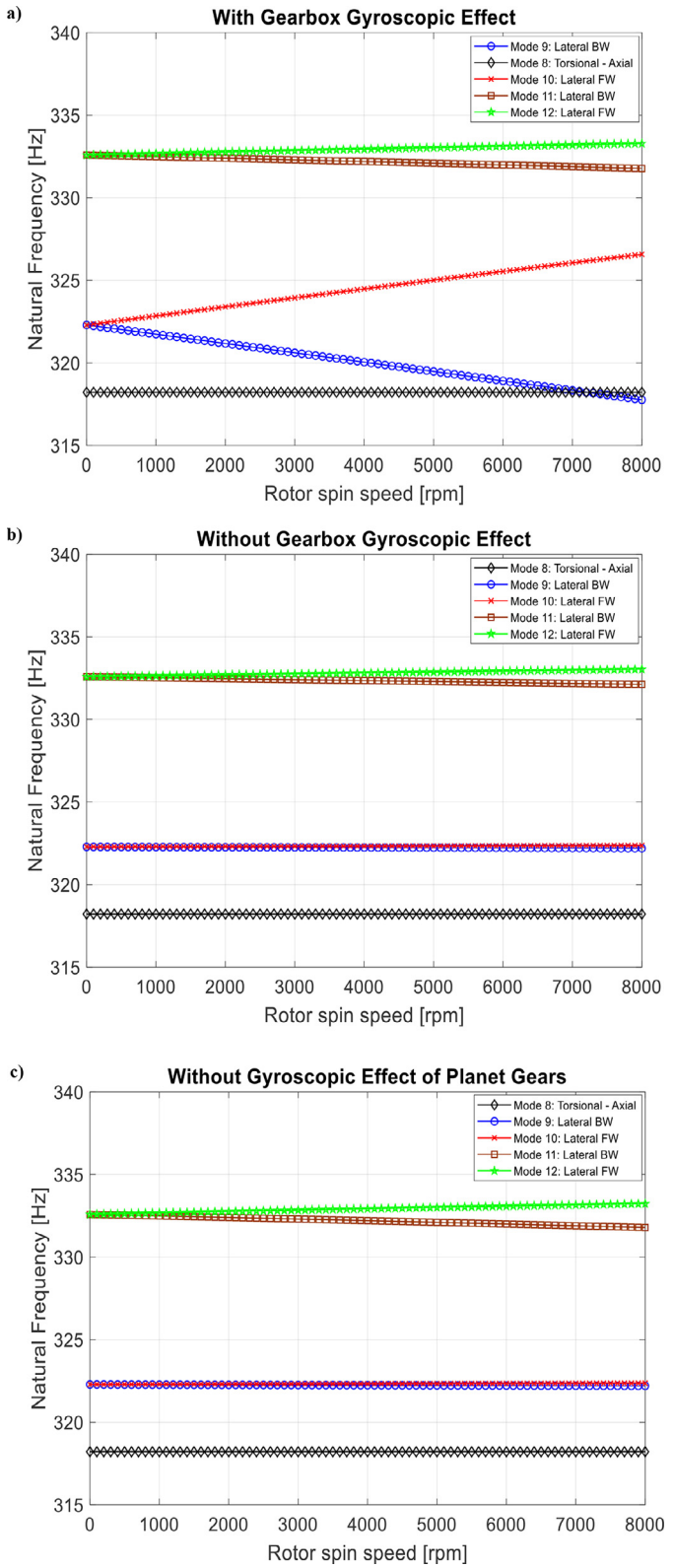

Fig. 11. Campbell diagram, a) with gearbox gyroscopic effect, b) without gearbox gyroscopic effect, c) without planet gear gyroscopic effect.

Table 5
Case studies for gyroscopic effects.

Gyroscopic Effects	With gearbox - Case A	Without gearbox - Case B	Without planet gears - Case C
Shafts	X	X	X
Ring Gear	X		X
Sun Gear	X		X
Planet Gears	X		
Carrier	X		X

As presented in Table 2, the gearbox has a higher energy at a value of 94% for the 9th (Lateral BW) and 10th (Lateral FW) modes, whereas a lower modal energy at a value of 17% for the 11th (Lateral BW) and 12th (Lateral FW) modes. It is important to point out that whole gearbox and planet gears can have significant gyroscopic effects at global system responses when they have higher modal energy in the vibration modes.

4. Conclusion

A comprehensive planet gear parameter study including the number of planet gears, planet mistuning, gear mesh stiffness, planet gear mass parameters and planet gear speed has been conducted on a hybrid dynamic model of planetary geared rotor systems in order to investigate the planet gear parameter effects on the natural frequencies and resulting mode shapes of helical and spur planetary geared rotors.

In general, the investigated parameters have varying impacts on both natural frequencies and mode shapes, which highlights the main original contributions of this paper and novelty of this research regarding planetary geared rotor design. The study of the number of planet gears reveals the reverse effect between the natural frequencies of the torsional-axial modes and the lateral modes. With an increase in the number of planet gears, the planetary gearbox becomes more rigid in the torsional-axial modes and more flexible in the lateral modes. Planet mistuning results in coupled lateral-torsional-axial modes for helical planetary geared rotors and coupled lateral-torsional modes for spur planetary geared rotors, which is due to the breaking cyclic symmetric structure of the planetary gearbox (unequally spaced planets). However, the natural frequency shifts due to planet mistuning are negligible. Furthermore, modal behaviours of both helical and spur planetary geared rotors are significantly affected by planet gear mass and gear mesh stiffness parameters. The torsional and coupled torsional-axial modes are more sensitive to the gear mesh stiffness, while the lateral modes are more sensitive to the planet mistuning and planet gear mass. The axial vibration modes, in general, are found to be less sensitive to the planet gear parameters. It is also found that planet gears have significant gyroscopic effects inside the planetary gearbox.

The three-dimensional dynamic model of a planetary geared rotor system used in this study shows that the mass and mesh stiffness parameters of the planet gears have significant effects on the modal behaviour of planetary geared rotors in terms of natural frequency shifts and mode shape changes. If a simple model of the planetary gearbox, which consists of mass and stiffness parameters, was used in this study instead of the complicated three-dimensional model, it might be able to capture the overall mass and stiffness parameters effect on the modal behaviour similar to the one shown in reference [62]. However, it would not be sufficient to estimate the effect of the planetary gearbox parameters, such as gear contact and planet gear parameters, on the global modal behaviour, since simple models do not include them in their formulations. Simple models assume that planetary gearboxes consist of a certain amount of mass/inertia and stiffness. They could be useful for the initial understanding of gearbox mass and stiffness effects.

To conclude, the presented results highlight the strong sensitivity of the vibration response on the planet gear parameters and the importance of investigating planet gear parameter effects on the modal behaviour of planetary geared rotor systems. The reader should note that although the presented quantitative results are specific to the system under investigation, the qualitative findings are more generically applicable for planetary geared rotor systems. Mechanical system designers can follow the main findings of this paper as general guidelines for the design of planetary geared rotor systems.

Data Availability

The data that has been used is confidential.

Acknowledgement

This study was funded by the Ministry of National Education of the Republic of Turkey under YLSY grant.

Appendix

Figs. A1, A2, A3

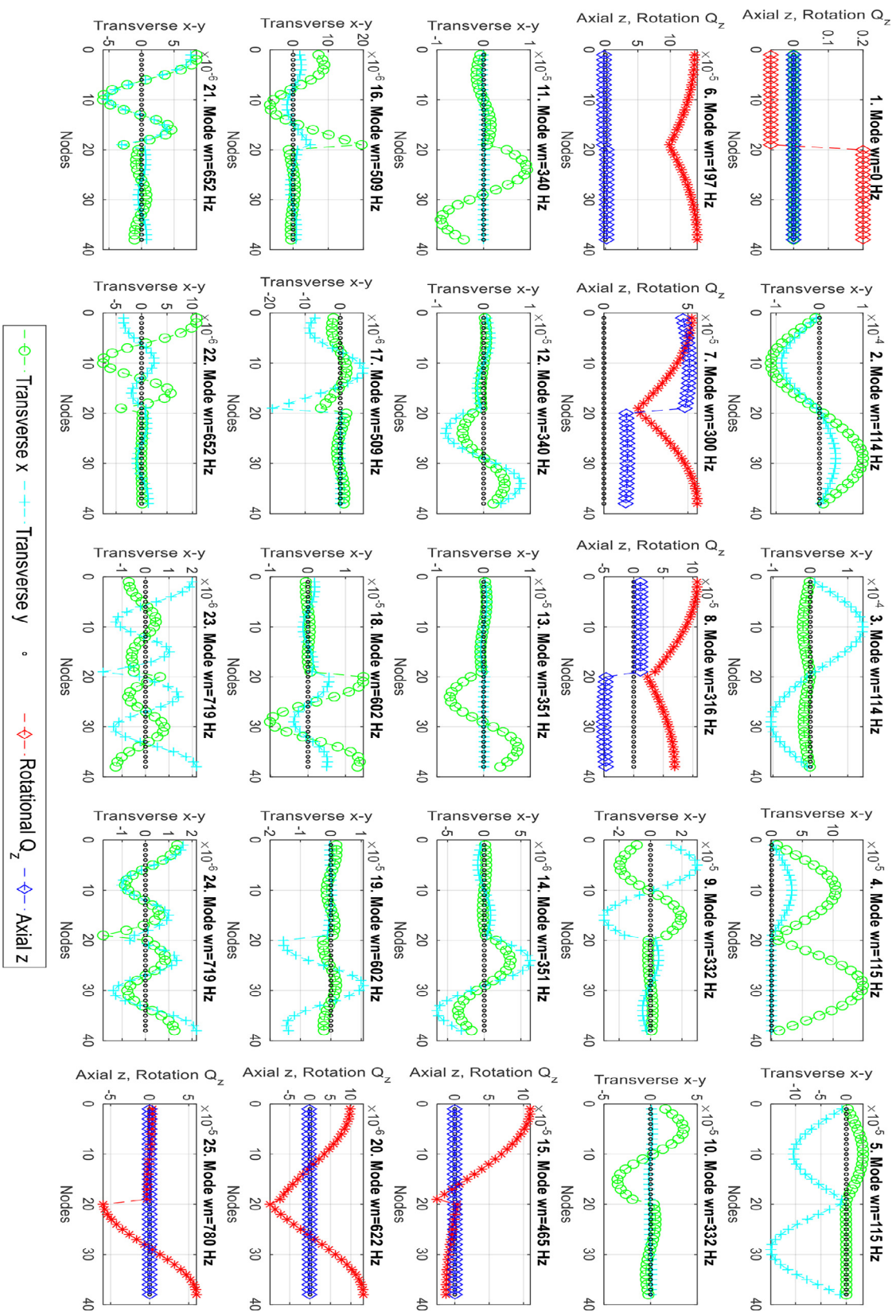

Fig. A1. Mode shapes of the helical planetary geared rotor with three planets.

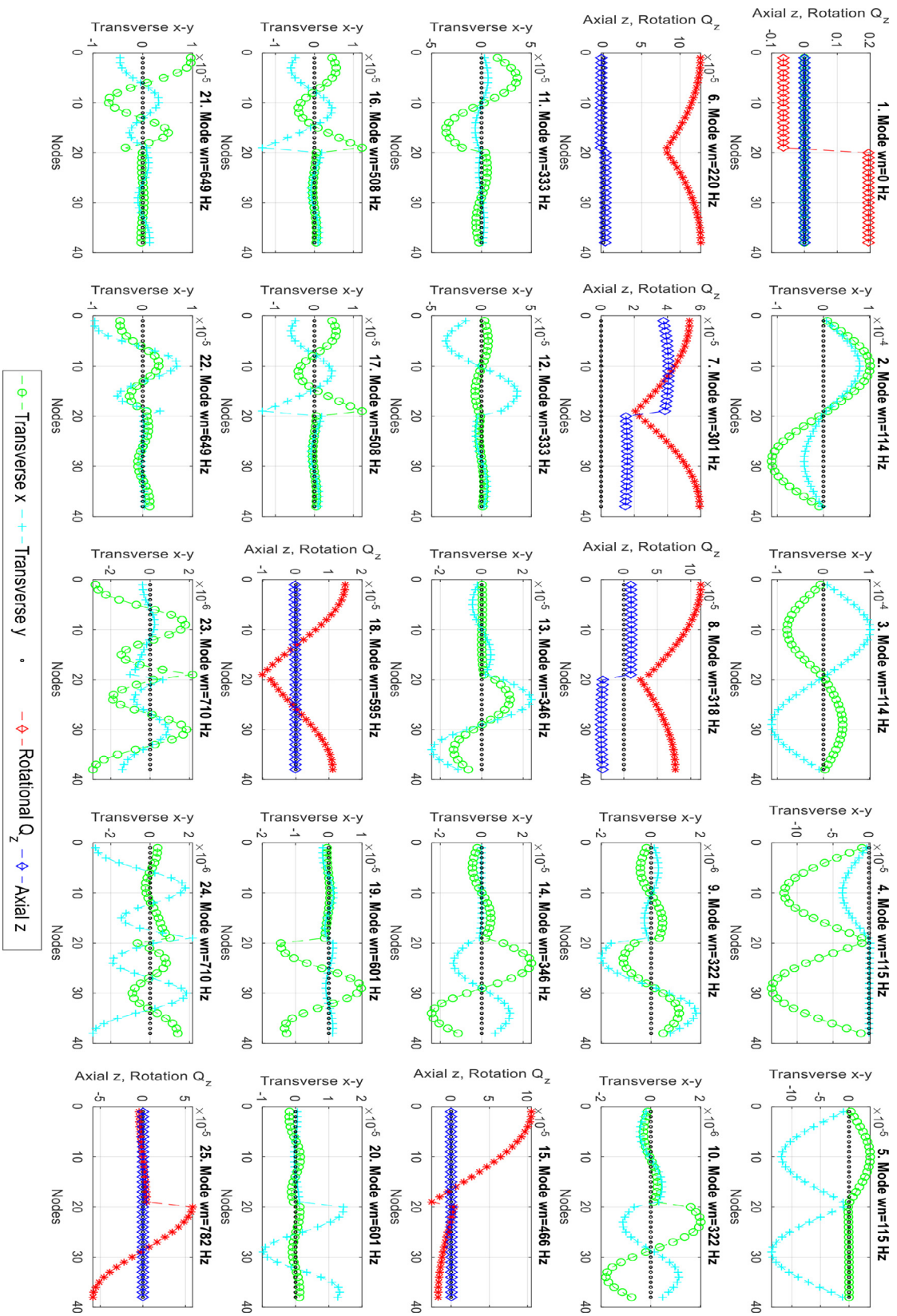

Fig. A2. Mode shapes of the helical planetary geared rotor with four planets.

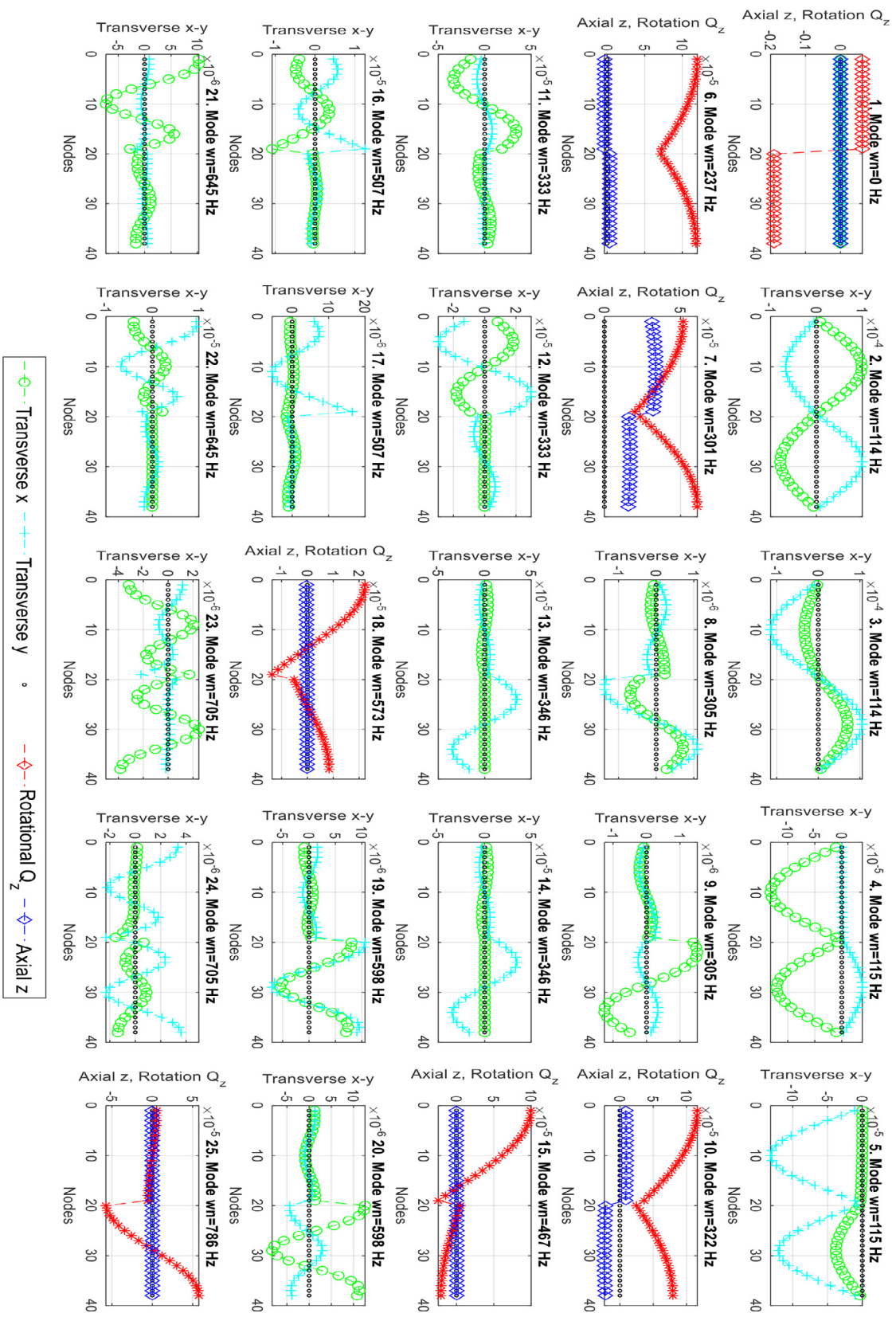

Fig. A3. Mode shapes of the helical planetary geared rotor with five planets.

References

[1] J. Wei, L. Shi, A. Zhang, D. Qin, Modeling and dynamic characteristics of planetary gear transmission in non-inertial system of aerospace environment, Proc. ASME Des. Eng. Tech. Conf. 10 (2019) 1–12, doi:10.1115/1.4045354.
[2] S. Wang, R. Zhu, Jin Feng, Study on load sharing behavior of coupling gear-rotor-bearing system of GTF aero-engine based on multi-support of rotors, Mech. Mach. Theory. 147 (2020) 103764, doi:10.1016/j.mechmachtheory.2019.103764.
[3] C. Liu, X. Yin, Y. Liao, Y. Yi, D. Qin, Hybrid dynamic modeling and analysis of the electric vehicle planetary gear system, Mech. Mach. Theory. 150 (2020) 103860, doi:10.1016/j.mechmachtheory.2020.103860.
[4] Z. Li, B. Wen, K. Wei, W. Yang, Z. Peng, W. Zhang, Flexible dynamic modeling and analysis of drive train for Offshore Floating Wind Turbine, Renew. Energy. 145 (2020) 1292–1305, doi:10.1016/j.renene.2019.06.116.
[5] T. Hidaka, Y. Terauchi, Dynamic behavior of planetary gear: 1st report load distribution in planetary gear, Bull. JSME. 19 (1976) 690–698.
[6] T. Hidaka, Y. Terauchi, K. Ishioka, Dynamic behavior of planetary gear: 2nd report, displacement of sun gear and ring gear, Bull. JSME. 19 (1976) 1563–1570.
[7] T. Hidaka, Y. Terauchi, M. Nohara, J. Oshita, Dynamic behavior of planetary gear: 3rd report, Displacement of ring gear in direction of line of action, Bull. JSME. 20 (1977) 1663–1672.
[8] T. Hidaka, Y. Terauchi, K. ISHIOKA, Dynamic behavior of planetary gear: 4th report, influence of the transmitted tooth load on the dynamic increment load, Bull. JSME. 22 (1979) 877–884.
[9] Y. Terauchi, K. Nagamura, Dynamic behavior of planetary gear: 5th report, dynamic increment of torque, Bull. JSME. 22 (1979) 1017–1025.
[10] T. Hidaka, Y. Terauchi, K. Nagamura, Dynamic behavior of planetary gear: 6th report, influence of meshing-phase, Bull. JSME. 22 (1979) 1026–1033.
[11] T. Hidaka, Y. Terauchi, K. NAGAMURA, Dynamic behavior of planetary gear: 7th report, Influence of the Thickness of the Ring Gear, Bull. JSME. 22 (1979) 1142–1149.
[12] R. August, R. Kasuba, Torsional vibrations and dynamic loads in a basic planetary gear system, J. Vib. Acoust. 108 (1986) 348–353, doi:10.1115/1.3269349.
[13] A. Kahraman, Natural modes of planetary gear trains, J. Sound Vib. 173 (1994) 125–130, doi:10.1006/jsvi.1994.1222.
[14] A. Kahraman, Free torsional vibration characteristics of compound planetary gear sets, Mech. Mach. Theory. 36 (2001) 953–971, doi:10.1016/S0094-114X(01)00033-7.
[15] M. Inalpolat, A. Kahraman, Dynamic modelling of planetary gears of automatic transmissions, Proc. Inst. Mech. Eng. Part K J. Multi-Body Dyn. 222 (2008) 229–242, doi:10.1243/14644193JMBD138.
[16] Y. Guo, R.G. Parker, Purely rotational model and vibration modes of compound planetary gears, Mech. Mach. Theory. 45 (2010) 365–377, doi:10.1016/j.mechmachtheory.2009.09.001.
[17] J. Lin, R.G. Parker, Analytical characterization of the unique properties of planetary gear free vibration, J. Vib. Acoust. 121 (1999) 316–321, doi:10.1115/1.2893982.
[18] L. Zhang, Y. Wang, K. Wu, R. Sheng, Q. Huang, Dynamic modeling and vibration characteristics of a two-stage closed-form planetary gear train, Mech. Mach. Theory. 97 (2016) 12–28, doi:10.1016/j.mechmachtheory.2015.10.006.
[19] D.C. Fyler, M. Inalpolat, A dynamic model for double-planet planetary Gearsets, J. Vib. Acoust. 138 (2016) 21006, doi:10.1115/1.4032181.
[20] F. Concli, L. Cortese, R. Vidoni, F. Nalli, G. Carabin, A mixed FEM and lumped-parameter dynamic model for evaluating the modal properties of planetary gearboxes †, J. Mech. Sci. Technol. 32 (2018) 3047–3056, doi:10.1007/s12206-018-0607-9.
[21] A. Saada, P. Velex, An extended model for the analysis of the dynamic behavior of planetary trains, J. Mech. Des. Trans. ASME. 117 (1995) 241–247, doi:10.1115/1.2826129.
[22] A. Kahraman, Planetary gear train dynamics, J. Mech. Des. 116 (1994) 713, doi:10.1115/1.2919441.
[23] T. Eritenel, R.G. Parker, Modal properties of three-dimensional helical planetary gears, J. Sound Vib. 325 (2009) 397–420, doi:10.1016/j.jsv.2009.03.002.
[24] P. Sondkar, A. Kahraman, A dynamic model of a double-helical planetary gear set, Mech. Mach. Theory. 70 (2013) 157–174, doi:10.1016/j.mechmachtheory.2013.07.005.
[25] V. Abousleiman, P. Velex, A hybrid 3D finite element/lumped parameter model for quasi-static and dynamic analyses of planetary/epicyclic gear sets, Mech. Mach. Theory. 41 (2006) 725–748, doi:10.1016/j.mechmachtheory.2005.09.005.
[26] J. Lai, Y. Liu, X. Xu, H. Li, J. Xu, S. Wang, W. Guo, Dynamic modeling and analysis of Ravigneaux planetary gear set with unloaded floating ring gear, Mech. Mach. Theory. 170 (2022) 104696, doi:10.1016/j.mechmachtheory.2021.104696.
[27] T.M. Ericson, R.G. Parker, Planetary gear modal vibration experiments and correlation against lumped-parameter and finite element models, J. Sound Vib. 332 (2013) 2350–2375, doi:10.1016/j.jsv.2012.11.004.
[28] A. Hammami, A.F. Del Rincon, F.V. Rueda, F. Chaari, M. Haddar, Modal analysis of back-to-back planetary gear: experiments and correlation against lumped-parameter model, J. Theor. Appl. Mech. 125 (2015), doi:10.15632/jtam-pl.53.1.125.
[29] A. Mbarek, A.F. Del Rincon, A. Hammami, M. Iglesias, F. Chaari, F. Viadero, M. Haddar, Comparison of experimental and operational modal analysis on a back to back planetary gear, Mech. Mach. Theory. 124 (2018) 226–247, doi:10.1016/j.mechmachtheory.2018.03.005.
[30] T.M. Ericson, R.G. Parker, Experimental measurement and finite element simulation of elastic-body vibration in planetary gears, Mech. Mach. Theory. 160 (2021) 104264, doi:10.1016/j.mechmachtheory.2021.104264.
[31] Y. Guo, R.G. Parker, Sensitivity of general compound planetary gear natural frequencies and vibration modes to model parameters, J. Vib. Acoust. 132 (2010) 11006, doi:10.1115/1.4000461.
[32] J. Lin, R.G. Parker, Sensitivity of planetary gear natural frequencies and vibration modes to model parameters, J. Sound Vib. 228 (1999) 109–128.
[33] H. Li, J. Liu, J. Ma, Y. Shao, Effect of the radial support stiffness of the ring gear on the vibrations for a planetary gear system, J. Low Freq. Noise, Vib. Act. Control. (2019) 146134841984464, doi:10.1177/1461348419844642.
[34] R.G. Parker, X. Wu, Vibration modes of planetary gears with unequally spaced planets and an elastic ring gear, J. Sound Vib. 329 (2010) 2265–2275, doi:10.1016/j.jsv.2009.12.023.
[35] Z. Cao, Y. Shao, M. Rao, W. Yu, Effects of the gear eccentricities on the dynamic performance of a planetary gear set, Nonlinear Dyn 91 (2018) 1–15, doi:10.1007/s11071-017-3738-0.
[36] A. Mbarek, A. Hammami, A. Fernandez Del Rincon, F. Chaari, F. Viadero Rueda, M. Haddar, Effect of load and meshing stiffness variation on modal properties of planetary gear, Appl. Acoust. 147 (2019) 32–43, doi:10.1016/j.apacoust.2017.08.010.
[37] T.M. Ericson, R.G. Parker, Natural frequency clusters in planetary gear vibration, J. Vib. Acoust. 135 (2013) 61002, doi:10.1115/1.4023993.
[38] C.G. Cooley, R.G. Parker, Vibration properties of high-speed planetary gears with gyroscopic effects, J. Vib. Acoust. 134 (2012) 61014, doi:10.1115/1.4006646.
[39] C.G. Cooley, R.G. Parker, Eigenvalue sensitivity and veering in gyroscopic systems with application to high-speed planetary gears, Eur. J. Mech. A/Solids. 67 (2018) 123–136, doi:10.1016/j.euromechsol.2017.09.003.
[40] J. Lin, R.G. Parker, Natural frequency veering in planetary gears, Mech. Struct. Mach. 29 (2001) 411–429.
[41] J.S. Rao, T.N. Shiau, J.R. Chang, Theoretical analysis of lateral response due to torsional excitation of geared rotors, Mech. Mach. Theory. 33 (1998) 761–783, doi:10.1016/S0094-114X(97)00056-6.
[42] S. Chen, J. Tang, Y. Li, Z. Hu, Rotordynamics analysis of a double-helical gear transmission system, Meccanica 51 (2016) 251–268, doi:10.1007/s11012-015-0194-0.
[43] A. Kahraman, H.N. Ozguven, D.R. Houser, J.J. Zakrajsek, Dynamic Analysis of Geared Rotors by Finite Elements, J. Mech. Des. 114 (1992) 507, doi:10.1115/1.2926579.

[44] H.N. Özgüven, A non-linear mathematical model for dynamic analysis of spur gears including shaft and bearing dynamics, J. Sound Vib. 145 (1991) 239–260, doi:10.1016/0022-460X(91)90590-G.
[45] S. Chowdhury, R.K. Yedavalli, Dynamics of low speed geared shaft systems mounted on rigid bearings, Mech. Mach. Theory. 112 (2017) 123–144, doi:10.1016/j.mechmachtheory.2017.02.002.
[46] S. Chowdhury, R.K. Yedavalli, Vibration of high speed helical geared shaft systems mounted on rigid bearings, Int. J. Mech. Sci. 142–143 (2018) 176–190, doi:10.1016/j.ijmecsci.2018.04.033.
[47] Z. Hu, J. Tang, S. Chen, D. Lei, Effect of mesh stiffness on the dynamic response of face gear transmission system, J. Mech. Des. 135 (2013) 71005, doi:10.1115/1.4024369.
[48] S. Chen, J. Tang, C. Zhou, Z. Hu, Modal and whirling analysis of coupled lateral and torsional vibration of herringbone gear, Int. J. Dyn. Control. 2 (2014) 404–414, doi:10.1007/s40435-013-0042-9.
[49] H.Y. Qi, L. Liu, Finite element analysis for vibration characteristic on gear rotors, Appl. Mech. Mater. 273 (2013) 193–197, doi:10.4028/www.scientific.net/AMM.273.193.
[50] H. Liu, Z. Zhan, Modal properties of a two-stage planetary gear system with a Timoshenko beam as the intermediate shaft model, Proc. Inst. Mech. Eng. Part D J. Automob. Eng. (2021) 95440702110192, doi:10.1177/09544070211019227.
[51] Y. Huangfu, J. Zeng, H. Ma, X. Dong, H. Han, Z. Zhao, A flexible-helical-geared rotor dynamic model based on hybrid beam-shell elements, J. Sound Vib. 511 (2021) 116361, doi:10.1016/j.jsv.2021.116361.
[52] J. Wang, R. Li, X. Peng, Survey of nonlinear vibration of gear transmission systems, Appl. Mech. Rev. 56 (2003) 309–329.
[53] A. Kahraman, R. Singh, Non-linear dynamics of a spur gear pair, J. Sound Vib. 142 (1990) 49–75, doi:10.1016/0022-460X(90)90582-K.
[54] D. Shin, A. Palazzolo, Nonlinear analysis of a geared rotor system supported by fluid film journal bearings, J. Sound Vib. 475 (2020) 115269, doi:10.1016/j.jsv.2020.115269.
[55] A. Hammami, A. Mbarek, A. Fernández, F. Chaari, F. Viadero, M. Haddar, Dynamic behavior of the nonlinear planetary gear model in nonstationary conditions, Proc. Inst. Mech. Eng. Part C J. Mech. Eng. Sci. 235 (2021) 4648–4662, doi:10.1177/0954406220941048.
[56] A. Muszynska, Rotordynamics, CRC Press, 2005, doi:10.1201/9781420027792.
[57] G. Genta, Dynamics of Rotating Systems, Springer Science & Business Media, 2007.
[58] M.I. Friswell, J.E.T. Penny, S.D. Garvey, A.W. Lees, Dynamics of Rotating Machines, Cambridge University Press, Cambridge, 2010, doi:10.1017/CBO9780511780509.
[59] J.S. Rao, History of Rotating Machinery Dynamics, Springer, Netherlands, Dordrecht, 2011, doi:10.1007/978-94-007-1165-5.
[60] Y. Ishida, T. Yamamoto, Linear and Nonlinear Rotordynamics, Wiley-VCH Verlag GmbH & Co. KGaA, Weinheim, Germany, 2012, doi:10.1002/9783527651894.
[61] W. Sun, X. Ding, J. Wei, A. Zhang, A method for analyzing sensitivity of multi-stage planetary gear coupled modes to modal parameters, J. Vibroengineering. 17 (2015) 3133–3146.
[62] A. Tatar, C.W. Schwingshackl, Effect of a planetary gearbox on the dynamics of a rotor system, in: ASME Turbo Expo 2018 Turbomach. Tech. Conf. Expo., American Society of Mechanical Engineers, Oslo, 2018, pp. 1–11.
[63] A. Tatar, C.W. Schwingshackl, M.I. Friswell, Dynamic behaviour of three-dimensional planetary geared rotor systems, Mech. Mach. Theory. 134 (2019) 39–56, doi:10.1016/j.mechmachtheory.2018.12.023.
[64] P. Wang, H. Xu, H. Ma, H. Han, Y. Yang, Effects of three types of bearing misalignments on dynamic characteristics of planetary gear set-rotor system, Mech. Syst. Signal Process. 169 (2022) 108736, doi:10.1016/j.ymssp.2021.108736.
[65] C.G. Cooley, R.G. Parker, A review of planetary and Epicyclic gear dynamics and vibrations research, Appl. Mech. Rev. 66 (2014) 40804, doi:10.1115/1.4027812.
[66] T.N. Shiau, J.S. Rao, J.R. Chang, S.-.T. Choi, Dynamic behavior of geared rotors, J. Eng. Gas Turbines Power. 121 (1999) 494–503.
[67] Y. Zhang, Q. Wang, H. Ma, J. Huang, C. Zhao, Dynamic analysis of three-dimensional helical geared rotor system with geometric eccentricity, J. Mech. Sci. Technol. 27 (2013) 3231–3242, doi:10.1007/s12206-013-0846-8.
[68] S. Zhou, Z. Ren, G. Song, B. Wen, Dynamic characteristics analysis of the coupled lateral-torsional vibration with spur gear system, Int. J. Rotat. Mach. 2015 (2015) 1–14, doi:10.1155/2015/371408.
[69] D.J. Inman, Engineering Vibration, Prentice Hall New Jersey, 2008.
[70] D.J. Ewins, Modal testing: theory, practice, and Application, Research Studies Press, 2000.
[71] A. Tatar, L. Salles, A.H. Haslam, C.W. Schwingshackl, Comparison of computational generalized and standard eigenvalue solutions of rotating systems, in: M. Mains, B.J. Dilworth (Eds.), Top. Modal Anal. Testing, Springer International Publishing, 2018 Vol. 9, doi:10.1007/978-3-319-74700-2.
[72] H. Dai, X. Long, F. Chen, C. Xun, An improved analytical model for gear mesh stiffness calculation, Mech. Mach. Theory. 159 (2021) 104262, doi:10.1016/j.mechmachtheory.2021.104262.
[73] Q. Wang, B. Zhao, Y. Fu, X. Kong, H. Ma, An improved time-varying mesh stiffness model for helical gear pairs considering axial mesh force component, Mech. Syst. Signal Process. 106 (2018) 413–429, doi:10.1016/j.ymssp.2018.01.012.
[74] H. Ma, J. Zeng, R. Feng, X. Pang, B. Wen, An improved analytical method for mesh stiffness calculation of spur gears with tip relief, Mech. Mach. Theory. 98 (2016) 64–80, doi:10.1016/j.mechmachtheory.2015.11.017.
[75] Y. Sun, H. Ma, Y. Huangfu, K. Chen, L. Che, B. Wen, A revised time-varying mesh stiffness model of spur gear pairs with tooth modifications, Mech. Mach. Theory. 129 (2018) 261–278, doi:10.1016/j.mechmachtheory.2018.08.003.
[76] C.G. Cooley, C. Liu, X. Dai, R.G. Parker, Gear tooth mesh stiffness: a comparison of calculation approaches, Mech. Mach. Theory. 105 (2016) 540–553, doi:10.1016/j.mechmachtheory.2016.07.021.
[77] C. Natali, M. Battarra, G. Dalpiaz, E. Mucchi, A critical review on FE-based methods for mesh stiffness estimation in spur gears, Mech. Mach. Theory. 161 (2021) 104319, doi:10.1016/j.mechmachtheory.2021.104319.
[78] P. Lynwander, Gear Drive systems: Design and Application, CRC Press, 1983.
[79] J.E. Shigley, Shigley's Mechanical Engineering Design, Tata McGraw-Hill Education, 2011.